

Influence of Pressure on the Radial and Tangential Penetration of Adhesive Resin into Poplar Wood and on the Shear Strength of Adhesive Joints

Ivana Gavrilović-Grmuša,^{a,*} Manfred Dunky,^{b,*} Milanka Djiporović-Momčilović,^a Mladjan Popović,^a and Jasmina Popović^a

This work deals with the influence of specific pressure during the press process on the radial and tangential penetration of urea-formaldehyde (UF) adhesive into poplar, as well as on the shear strength of lap joints prepared at these different pressures. An epi-fluorescence microscope was used for measuring the adhesive penetration when investigating microtome slides (20- μm thick) cut from the joint samples. The average penetration depth (d_{ap}) and the size of the interphase region (l) increased with the increase of pressure from 0.5 to 1.0 N/mm². Further increase in the pressure to 1.5 N/mm² did not produce a significant change in d_{ap} or l . On the contrary, the area of filled lumens and rays (A) showed a steady decrease as the specific pressure increased. Such behavior influenced the filled interphase region (h), which also decreased with increased pressure. Tangential samples (radial penetration) obtained higher values of lap shear strength and showed less dependence on the specific pressure than the radial samples (tangential penetration). Higher shear strength based on radial penetration corresponded to the thicker interphase region of these samples. The highest shear strength for both directions of penetration was obtained for the specific pressure of 1.0 N/mm².

Keywords: Penetration; Poplar; Urea-formaldehyde adhesive; Microscopy; Shear strength

Contact information: a: University of Belgrade - Faculty of Forestry, Kneza Višeslava 1, 11030 Belgrade, Serbia; b: Kronospan GmbH Lampertswalde, D-01561 Lampertswalde, Germany;
* Corresponding authors: ivana.grmusa@sfb.bg.ac.rs; m.dunky@kronospan.de

INTRODUCTION

Penetration can be defined as the ability of an adhesive to enter into the lumen and into cell walls *via* a process of fluid movement (Marra 1992). Adhesive penetration into wood occurs (i) on the micrometer level as hydrodynamic flow and capillary action through the large voids into the porous and capillary structure of wood (bulk penetration); it mostly fills cell lumens, as well as fractures and surface debris caused by processing (Marra 1992); and (ii) on the sub-micrometer level as diffusion penetration into cell walls and micro-fissures through the micro voids within the wood cell walls (Johnson and Kamke 1992).

The interphase region of the adhesive bond as the zone of bulk penetration of the adhesive comprises wood and adhesive; penetration is determined (i) by wood-related parameters (such as the diameter of the lumen and exposure on the wood surface due to grain slope); (ii) by the properties of the resin and adhesive mix (such as chemical structure like molar mass distribution, composition of the adhesive mix, viscosity and surface energy, amount of adhesive spread, hardening time, and rate of resin curing); and

(iii) by bonding processing parameters (such as assembly time, press temperature and pressure, or moisture level) (Gavrilovic-Grmusa *et al.* 2010a). Hydrodynamic flow, especially, is initiated by the external compression force applied to the wood surfaces to be bonded. By forming the interphase, the adhesive bulk penetration strongly determines the bonding effect. Though mechanical interlocking is not the main reason for bonding, an adequate penetration of the resin into the wood surface as a porous network of interconnected cells enables the formation of a sufficiently large bonding interface as a two-dimensional contact area between the molecules of wood and adhesive and helps in creating strong bonds (Marra 1992; Wang and Yan 2005). At any rate, the main part of penetration must take place before the curing of the resin begins.

Usually, because of their greater molar masses, the penetration of adhesives involves the filling of the lumens by bulk penetration rather than cell wall penetration (Gindl *et al.* 2003; Konnerth *et al.* 2008). To investigate cell wall penetration, Gindl *et al.* (2003) used a low molar mass impregnation resin, which on the other side cannot be used as an adhesive resin because of the risk of over-penetration.

Bulk penetration is highly controlled by the size of the molecules, with easier access by low molar mass adhesives; this effect is additionally enhanced by the decrease in viscosity due to the increasing temperature in a bond line during hot pressing. The molecules with higher molar mass preferably remain at the wood surface.

Adhesive penetration into hardwood is likely to be dominated by flow into vessel elements. Poplar has transport elements with wide lumens (vessels), surrounded by mechanical elements with far narrower lumens (by a factor of 3 to 5) and lignified walls with cracked pits. The vessels amount for only 27% of the total mass of the xylem, while the mechanical elements (wood fibers) comprise up to 70%. Penetration into poplar is characterized by significantly higher adhesive penetration depths compared with hardwoods with higher density or with fir, despite the similar porosity of poplar and fir, because of the different anatomical structure of these species resulting in different mechanisms of penetration (Gavrilovic-Grmusa *et al.* 2012b).

Low bond strengths result from either under- or over-penetration. Under-penetration means that the adhesive is not able to move into the wood substance enough to create a large active bonding surface (interface) within the interphase, and hence strong interaction between the wood and the adhesive. Over-penetration means that a big portion of the adhesive can penetrate the wood substance, causing starved joints as an insufficient amount of adhesive remained in the bond line to bridge the wood surfaces and to establish bond strength.

Furthermore, the bond strength between two wooden surfaces is determined by wood-related parameters (such as density, strength of the wood tissue, or grain angle), by the properties and penetration behavior of the resin, the adhesive mix, and the bonding processing parameters. The viscosity of the adhesive, especially in dependence of the temperature in the bond line during the press cycle, has to be adjusted by proper composition and molecular structure (molar mass distribution, degree of condensation) of the adhesive (Ellis and Steiner 1992). Additionally, the applied pressure influences the penetration, causing increased and deeper movement of the adhesive from the surface into the wood tissue.

In a series of papers, Gavrilovic-Grmusa *et al.* (2010a,b; 2012a,b) investigated (i) the penetration of urea formaldehyde (UF) resins of different molecular structure (size of the adhesive molecules, degree of condensation) into various wood species, as well as (ii) the achievable bond strengths (shear strengths).

The degree of condensation, especially, is one of the most important characteristics of a condensation resin and determines several properties of the resin (Dunky 2003).

The determination of the extent of lumen penetration into the wood structure is preferably performed by the examination of the cross-section of a bond line. This can be done using several microscopic methods, including light microscopy (Niemz *et al.* 2004; Singh *et al.* 2008; Nuryawan *et al.* 2014; Mahrtdt *et al.* 2015), transmitted end-reflected microscopy, fluorescence microscopy, epi-fluorescence microscopy (Edalat *et al.* 2014), (fluorescence) confocal laser scanning microscopy (CLSM) (Singh *et al.* 2008), scanning electron microscopy (SEM) (Niemz *et al.* 2004; Singh *et al.* 2008), transmission electron microscopy (TEM), SEM in combination with an energy-dispersive analyzer for X-rays (SEM/EDAX, TEM-EDXS) (Singh *et al.* 2015), X-ray microscopy, neutron radiography (Niemz *et al.* 2004), and autoradiography; for further references see Gavrilovic-Grmusa *et al.* (2010a).

Micro-tomography facilitates the sample preparation when investigating the penetration of various adhesives into wood (Hass *et al.* 2009, 2012; Evans *et al.* 2010; Modzel *et al.* 2011; Gavrilovic-Grmusa *et al.* 2012c; Paris *et al.* 2013, 2014; Kamke *et al.* 2014).

Pressure has two main functions in bond formation: to bring surfaces together, and to aid in the penetration and wetting of the adhesive (Marra 1992). Though it is general experience that the applied pressure enhances resin penetration (under consideration of all other factors influencing penetration), surprisingly, only very little information is available in the literature on the quantitative evaluation of resin penetration as a consequence of applied pressure. Brady and Kamke (1988) mentioned that pressure may increase penetration because it is the driving force behind hydrodynamic flow. However, little evidence of consolidation pressure influencing the penetration of a PF resin into aspen was found. The authors suspected that flow parallel to the bond line may have overruled the effect of pressure towards an enhanced penetration, especially at low moisture contents and at higher pressure; higher moisture content in the bond line before pressing then promotes penetration rather than spreading.

According to White (1977), pressure affected the depth of penetration of an adhesive into wood in different modes for earlywood and latewood. Because of the low porosity of latewood, pressure may squeeze out the resin laterally rather than causing deeper penetration; for the more porous earlywood, the depth of penetration tended to increase slightly as the pressure increased.

Sernek *et al.* (1999) reported that the penetration of an UF resin was enhanced by the application of pressure during the bonding process. By contrast, in the absence of an applied pressure, no differences were noticed between radial and tangential penetration into beech. The radial penetration was higher compared with penetration in the tangential direction when applying pressure; the increase was approximately 50% at the parallel lamination of solid-sawn beech wood, but up to nearly ten times at the cross-lamination of rotary-peeled beech veneers.

The objective of this study was therefore the evaluation of the influence of the pressure applied during the press cycle on the distribution of an UF resin within the wood substance by means of microscopic investigation.

EXPERIMENTAL

Urea Formaldehyde (UF) Resins

A laboratory UF resin with a rather low degree of condensation (DOC) according to a recipe described in the literature (Pizzi 1999) was prepared. This resin is the version with the lowest DOC in the series (UF I to UF III) as described by Gavrilovic-Grmusa (2010a), with a viscosity of 218 mPa·s, and is therefore referred to as “UF I” throughout this paper; the molar ratio formaldehyde to urea (F/U) was 2.0, with no extra urea added after the condensation step. This high molar ratio was selected in order to avoid any addition of urea after the acidic condensation step and, hence, the existence of low molar mass moieties in the resin, which would behave differently from the condensed part of the resin concerning their penetration behavior.

The adhesive mix applied onto the wood surfaces was prepared by the addition of 10 mass (%) of wheat flour as an extender and 0.05 mass (%) of Safranin as a marker to the liquid resin UF I (both numbers are based on solid resin). The addition of ammonium sulfate as a hardener to resin UF I was 0.5%, expressed as a solid hardener based on resin solids. Table 1 summarizes the characteristics of the resin UF I and the adhesive mix (including wheat flour, Safranin, and the hardener).

Table 1. Characteristics of the UF Resin UF I and the Adhesive Mix

Property	Unit	UF I	
		Resin	Adhesive mix
Solid content	%	53.7	54.4
Brookfield viscosity (20 °C)	mPa·s	218	545
Gel time	s	58	59

Preparation of the Bonded Joints and Preparation of Microtome Slices

The poplar log was cut from the trunk at a height of 1.3 m. Boards of 42-mm thickness were cut using a band-saw. After initial air drying, the boards were further dried in a laboratory kiln drier and planed to final dimensions of 1000 mm x 150 mm x 30 mm. These boards were then cut into radial and tangential blocks of 100 mm x 30 mm x 5 mm in order to obtain tangential and radial surfaces for the penetration investigations and for bonding for the shear strength tests (Fig. 1). The majority of the poplar blocks were taken from sapwood.

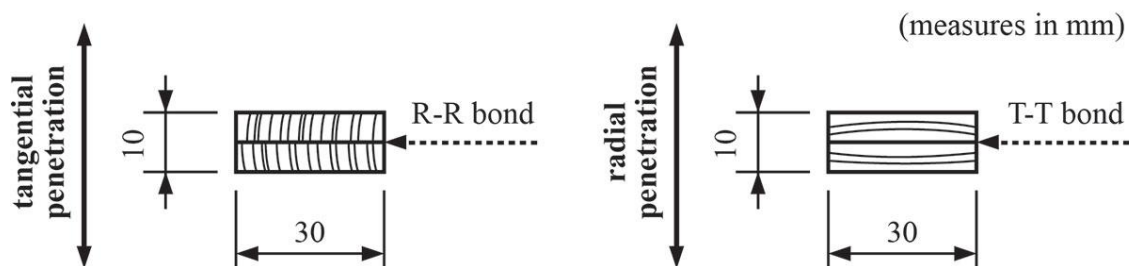


Fig. 1. Scheme of bonded samples for penetration tests and shear strength tests, with the bond line between two radial or two tangential plies; all measurements are in mm (Gavrilovic-Grmusa *et al.* 2012a)

Before bonding, the blocks were conditioned in a standard climate ($T = 20 \pm 2 \text{ }^\circ\text{C}$ and $\phi = 65 \pm 5\%$), yielding moisture contents (MC) of approximately 10%.

Assembling was performed following parallel to the grain directions, with the adhesive applied only to the block in the upper position of the joint; this should help to improve the penetration into the bottom block. The loading level of the UF adhesive mix was 200 g/m^2 . Five bonding samples were pressed at the same time in a hydraulic press at $120 \text{ }^\circ\text{C}$ and at different specific pressures ($0.5 \text{ resp. } 1.0 \text{ resp. } 1.5 \text{ N/mm}^2$) for 15 min. After hot pressing, the bonded samples were conditioned again in a standard climate before performing the various investigations.

Three microtome test specimens ($20\text{-}\mu\text{m}$ thick and with side lengths of 10 mm) were prepared from each joint sample at various positions on the transversal plane by a sliding microtome apparatus, exposing the bond line within the cross-sectional surface of the two jointed blocks.

Determination of Penetration

From each of the microtome slides (Fig. 2), five photos (with a 1.4-mm width on each photo) were taken at different positions along the bond line using epi-fluorescence microscopy (LEICA DM LS); so in total, approximately 7 mm of the whole width of the bond line of 10 mm in the microtome slide was investigated. The used set of optical filters consisted of a 450-nm excitation filter, a 510-nm dichromatic mirror, and a 515-nm emission filter. The image analysis system included a color video camera (LEICA DC 300) and an image processor with analysis software (IM1000 by LEICA Microsystems, Heerbrugg, Switzerland). These photos were then evaluated for penetration of the UF resin adhesive.

The individual depths of penetration (μm) were determined from each photograph of the microtome slides at 45 positions within the $1400\text{-}\mu\text{m}$ width of the bond-line shown (see positions over the whole width indicated with number 1 to 45). The depth of penetration here is defined as the sum of the distances the resin could penetrate the two blocks starting from the geometric center of the bond line (Fig. 2).

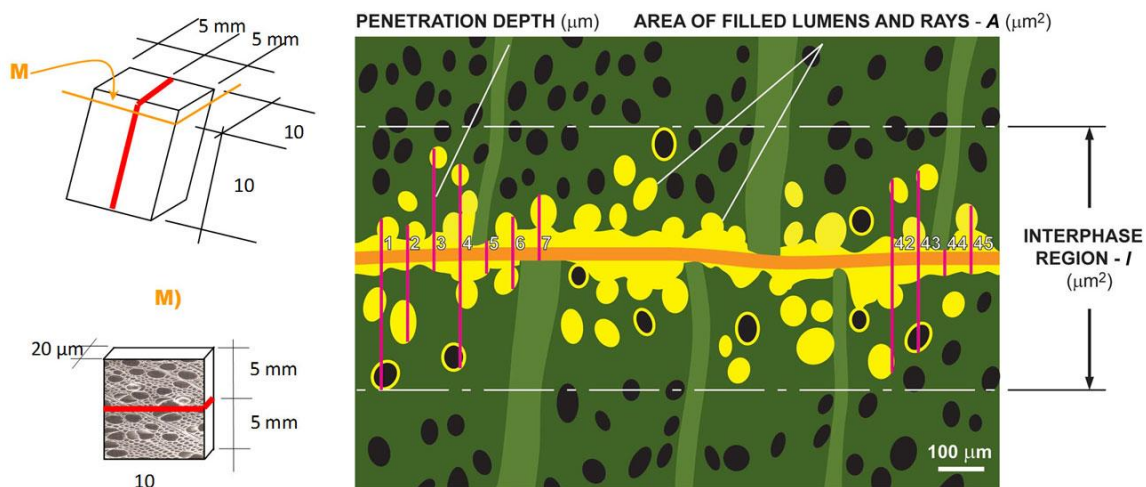


Fig. 2. Scheme of microtome specimens (M); the thick red line indicates the bond line. Right side: scheme of determination of A and I at the 45 positions indicated with number 1 to 45 (Gavrilović-Grmuša *et al.* 2012a)

Based on the individual depths of penetration (μm), several characteristic values were evaluated:

- a) average penetration depth (d_{ap}): mean value of penetration depths (μm)
- b) maximum individual penetration depth (d_{max} ; μm) within the investigated bond line
- c) ratio maximum to average penetration depth ($d_{\text{max}}/d_{\text{ap}}$)
- d) total interphase region (I , mm^2): I is calculated as the maximum individual penetration depth (d_{max}) multiplied by the width of the investigated bond line (1.4 mm). I includes the unfilled lumen area and the area of all filled lumens or filled rays (A), as well as all wood material cross-sections;
- e) area of all filled lumens and filled rays (A): determined from the photomicrographs by summarizing all filled lumens and rays;
- f) filled interphase region (I_f): expressed as the percentage A/I (%).

No separate evaluation for the two joined blocks was performed during the evaluation of d_{ap} and I_f , even though there may have been some difference in the individual penetration (i) between the block where the adhesive mix was applied and the block without application of adhesive mix, or (ii) especially if different portions of earlywood or latewood were given in the two blocks. Higher penetration into earlywood than into latewood was observed in a former paper for the radial penetration into fir and beech (Gavrilovic-Grmusa *et al.* 2010a).

Several microtome slides also were examined with a fluorescence confocal laser scanning microscopy (CLSM), as well as scanning electron microscopy (SEM); the details are described elsewhere (Gavrilovic-Grmusa *et al.* 2010a).

Testing of the Shear Strength

The lap shear tests were conducted according to EN 205 on a hydraulic test machine (ZWICK, Germany) at 6 mm/min in tensile mode. The failure zone was examined using a light microscope to determine the proportion of wood failure and the thickness of the wood layer in the wood failure. Ten replications were performed for each set of parameters.

Statistical Analysis

The statistical analysis was performed using both ANOVA and t-test, with the significance level of 5%. The single factor ANOVA was used for the analysis of the variances between the multiple test series, while the t-test was used for the comparison of the mean values between two test series.

RESULTS AND DISCUSSION

Photo-Micrographs of the Penetration into Poplar at Various Pressures

Figure 3 shows characteristic epi-fluorescence microphotographs of radial and tangential penetration for the adhesive mix of UF I into poplar at three different applied pressures. The light-colored sections on both sides of the bond line represent the UF

adhesive mix, which had penetrated to a certain extent into the wood material. Depending on the anatomical structure of poplar, the adhesive mix mainly filled the lumens of the vessels, as well as the rays. Only bulk penetration was investigated and evaluated, but not wood cell penetration.

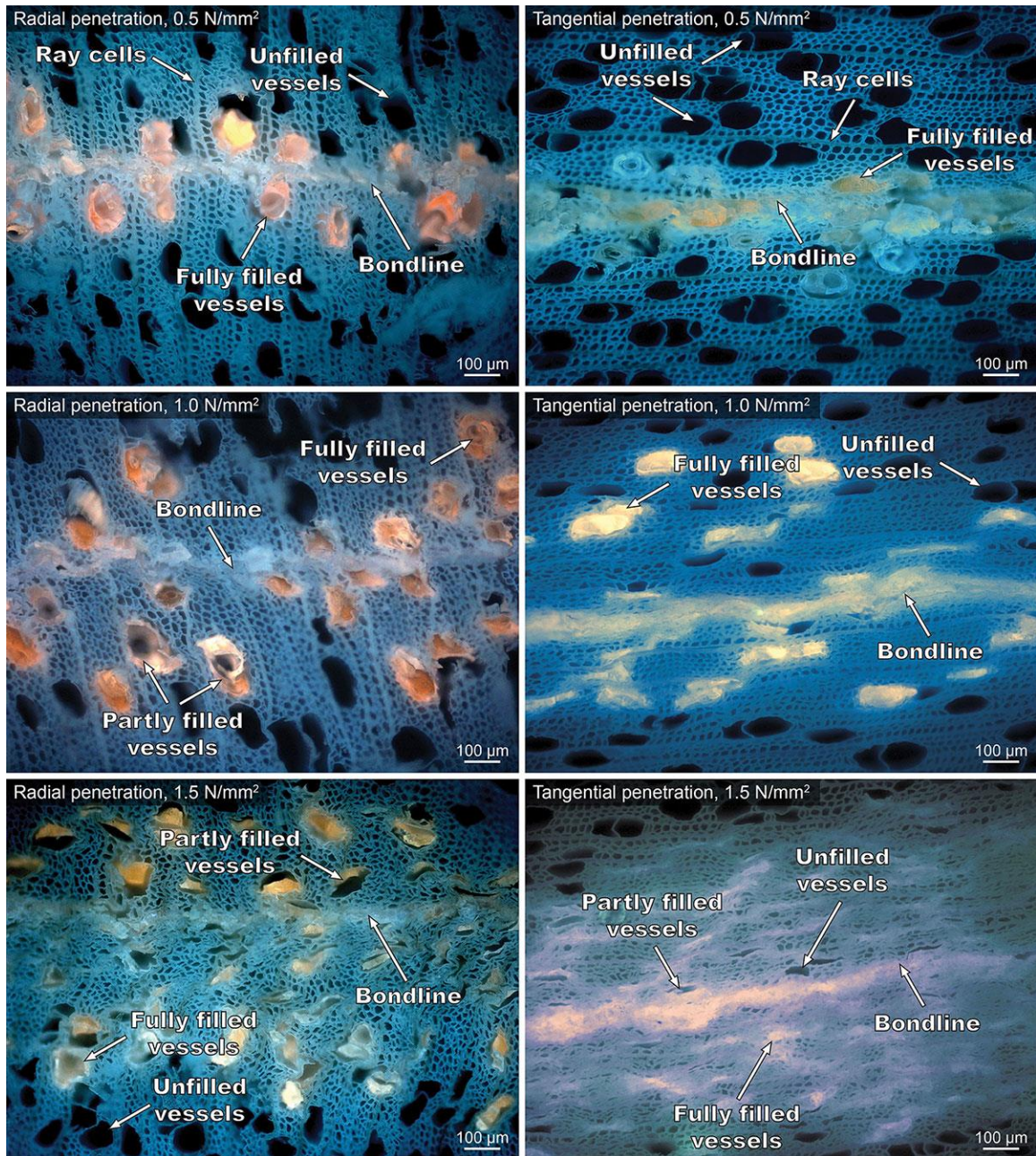


Fig. 3. Example of epi-fluorescence microphotograph with the penetration of UF resin I into poplar at three different pressures applied during the press cycle: 0.5 N/mm² (lowest level of pressure; top), 1.0 N/mm² (middle), and 1.5 N/mm² (highest level of pressure; bottom) for radial (left) and tangential penetration (right)

The left side shows the radial penetration (into the two tangential surfaces). Low pressure (Fig. 3, on top) left the bigger part of the resin in the bond line, with rather low penetration depth. At higher applied pressures (Fig. 3, middle and bottom), the resin penetrated the wood tissue much further, away from the geometrical bond line. At the highest pressure used in the work reported here, already significant changes in the wood cell structure occurred, caused by the pressure and supported by the plasticizing effects of heat and moisture; the lumens of poplar (vertical ellipses in the microphotograph, orientated preferably with their longer axis in the radial direction) were already crushed; this effect only occurs in the section of the interphase that is close to the geometrical bond line. Further away from the bond line (but still within the interphase), the structure of the wood tissue did not change; here also partly or fully filled lumens with the original structure and size can be seen.

The same effect, but much stronger, influenced by high pressure can be seen on the right side in Fig. 3, which shows microphotographs for the tangential penetration into radial surfaces (low pressure on top; highest pressure on bottom). Again, the depth of penetration increased at higher applied pressures. The effect of changing the wood cell structure is much stronger in the tangential direction of the pressure application; the elliptic lumens (orientated with their longer axis in radial direction) were reduced significantly in size by narrowing the cell walls parallel to the longer axis to each other; more or less all the lumens, including the adhesive, were strongly compressed.

Penetration Data of UF Resin (UF I) into Poplar at Various Pressures

Table 2 summarizes the penetration data for the UF resin (UF I) and poplar for the three applied pressures and the two directions of penetration.

Table 2. Penetration Characteristics of UF resin (UF I) into Poplar: Average Penetration Depth (d_{ap}); Maximum Penetration Depth (d_{max}); d_{max}/d_{ap} ratio; Average Size of the Interphase Region (l); Average Size of Filled Lumens and Rays within the Interphase Region (A); and Filled Interphase Region ($f=A/l$)

Poplar UF I	Pressure (N/mm ²)	d_{ap} (μ m)	d_{max} (μ m)	d_{max}/d_{ap}	l (mm ²)	A in l (mm ²)	f (%)
TT	0.5	185 ± 18	646	3.5 ± 0.40	0.91 ± 0.09	0.25 ± 0.03	27 ± 3.4
	1.0	324 ± 97	825	2.5 ± 0.48	1.15 ± 0.31	0.23 ± 0.04	21 ± 6.0
	1.5	331 ± 43	861	2.6 ± 0.47	1.21 ± 0.20	0.21 ± 0.05	18 ± 3.8
RR	0.5	210 ± 39	607	2.9 ± 0.50	0.85 ± 0.04	0.25 ± 0.02	29 ± 2.1
	1.0	355 ± 154	701	2.0 ± 1.38	0.98 ± 0.24	0.23 ± 0.03	23 ± 8.1
	1.5	341 ± 73	693	2.0 ± 0.42	0.97 ± 0.16	0.19 ± 0.03	20 ± 3.0
TT=Two tangential surfaces bonded (radial penetration) RR=Two radial surfaces bonded (tangential penetration)							

The average penetration depth (d_{ap}) (μ m) of UF resin I into poplar increased significantly when increasing the specific pressure from 0.5 to 1.0 N/mm², but it leveled out at the highest specific pressure with no statistical significance between 1.0 and 1.5 N/mm² of applied pressure (Fig. 4). This effect can be caused by two reasons. As long as there is enough resin available in the bond line when starting the press procedure, the higher pressure forces the adhesive to penetrate the wood tissue. This penetration is more complete and deep with an increase of external pressure onto the bond line. Due to the increase in temperature in the bond line and the decrease of the viscosity, this penetration

is accelerated for a certain time span. The average penetration is higher at the medium pressure compared to the lowest pressure, but does not increase further at the highest pressure; obviously the speed of penetration into the wood tissue is already at its maximum at this medium pressure during the time span before hardening of the resin slows down and finally stops liquid movement.

The flow paths become closer with higher external pressure due to the densification of the wood substance, as can be seen in the photomicrographs in Fig. 3. This effect slows down the movement of the adhesive resin during the time span until the chemical hardening of the resin takes place.

Tangential penetration was slightly higher at all pressure steps, but the difference from radial penetration was not significant.

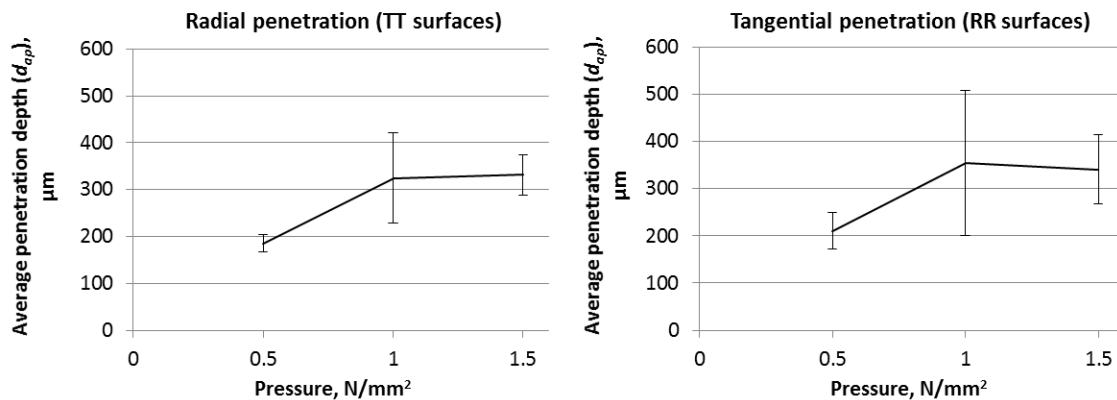


Fig. 4. Average penetration depth (d_{ap}) (μm) for poplar and UF resin I as a function of the specific pressure during the press process

The interphase region (I) was determined by the maximum individual penetration depth (d_{max}), as shown in Fig. 5, by multiplication by the width of the investigated bond line. Since this observed width has a constant value (1,400 μm), the statistical evaluation for I (Table 2) was identical to d_{max} .

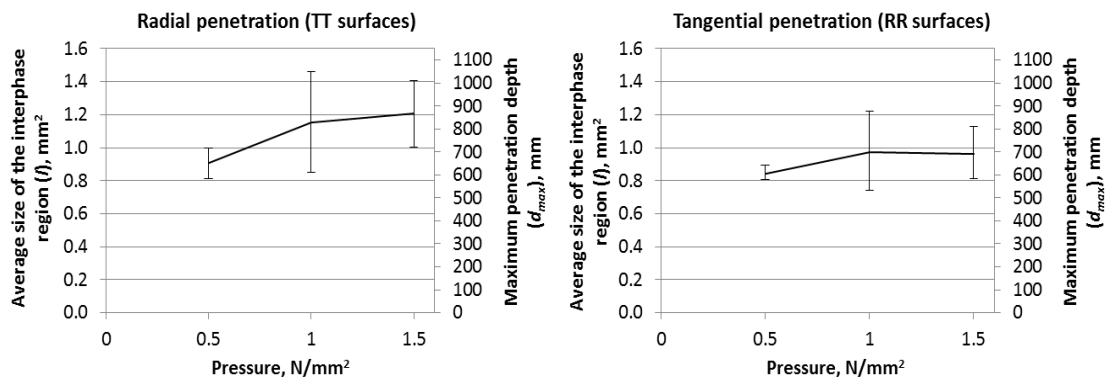


Fig. 5. Average size of the interphase region (I) (mm^2) and the maximum penetration depth (d_{max}) (μm) for poplar and UF resin I as a function of the specific pressure during the press process. The data shown belong to both y-axes, once expressed as I (at the left side) and once as d_{max} (at the right side)

Both I and d_{\max} apparently increase with the increase in pressure; the statistical difference only was given for the radial direction between the two lower pressures, but not for the tangential penetration (RR samples).

In addition, both values are higher in the radial direction than in the tangential direction, which is contrary to d_{ap} ; however, this difference is significant only for the highest pressure applied (1.5 N/mm²). In the radial direction, single flow paths enable deep penetration; this means that the resin is distributed in a broader layer (interphase); contrary to this, the resin distribution in the tangential direction yields in a narrower interphase, but with higher average penetration depth.

It is interesting to notice that for the applied pressure range (0.5 to 1.5 N/mm²), the d_{ap} increased by approximately 70%, whereas the d_{\max} increased by only by 15% (for TT) and 28% (for RR). Therefore, the ratio between the maximum and the average penetration depth (d_{\max}/d_{ap}) was introduced as a new parameter. This ratio decreased significantly between the two first pressure levels, and then leveled out (Fig. 6). The increased compression of wood tissue with a higher specific pressure may have had a particular effect on the vessels, which in poplar are characterized by wide lumens and relatively thin walls (Fig. 3). The higher pressure levels, with the consequence of higher overall resin penetration, obviously compressed the vessels, decreasing their cross-section enough to hinder extreme penetration through the individual flow paths. However, the lowest specific pressure applied did not affect the wood cells to a greater extent, thus leaving a higher number of vessels unaltered and therefore open for a certain portion of the UF resin to penetrate further away from the bond line. This different behavior at various pressure levels seems to have caused the reported changes of the d_{\max}/d_{ap} ratio.

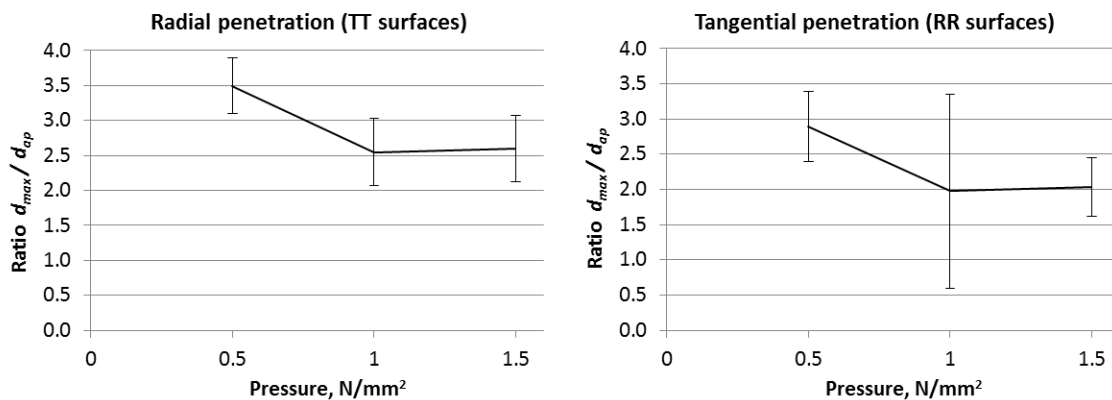


Fig. 6. Ratio of maximum and average penetration depths (d_{\max}/d_{ap}) for poplar and UF resin I as a function of the specific pressure during the press process

Similarly to the I and d_{\max} values, the d_{\max}/d_{ap} ratio increased 17% to 32% more in the radial direction (TT samples) than in the tangential direction (RR samples); the differences between the d_{\max}/d_{ap} in the radial and tangential directions were statistically significant for all pressure levels applied. The same explanation given for the IR and MP can be also valid for the d_{\max}/d_{ap} ratio; it can be suggested that the conformation of poplar vessels with the pits positioned on the radial walls enabled higher and more uniform adhesive penetration in the tangential direction. On the other hand, the d_{\max}/d_{ap} ratio was

higher in the radial direction due to the higher penetration depth throughout the individual flow paths.

The average size of the filled lumens and rays within the interphase (A) decreased slightly with higher specific pressures applied during the press process; however, there were no statistically significant differences between all the pressure levels (Fig. 7).

No difference was given between the two penetration directions; the slightly lower value for A for tangential penetration at the highest pressure was not significantly secured.

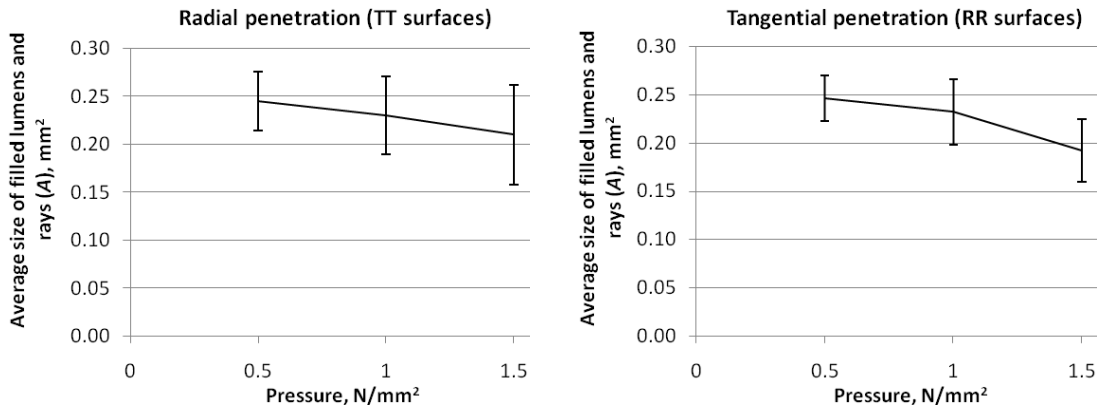


Fig. 7. Average size of filled lumens and rays within the interphase (A) (mm²) for poplar and UF resin I as a function of the specific pressure during the press process

The reason for the decrease of A under higher pressure is not fully clear; on the one hand, the anatomical structure of poplar wood elements has to be taken into consideration; the transport vessels especially have wide lumens and relatively thin walls; this enables a relatively higher penetration of the adhesive. It is also the case that many of the transport vessels are only partially filled with the adhesive. Under higher pressures, such vessels are quite easily compressed and thus decreased in volume, whereas the wide original lumens enable high penetration, and a certain compression of the vessels can already hinder penetration of the adhesive. The change in the size and shape of the lumens can also slightly falsify the determination of A by preventing the clear distinction between fully and only partially filled lumens.

Another effect was that because of the applied pressure, a somewhat stronger flow and, hence, even squeezing out of the adhesive in the bond line can occur.

The filled interphase region (I_f) describes the proportion of the filled cells within the interphase; as the thickness of the interphase (determined by d_{\max}) increased with higher specific pressure applied during the press process, the I_f decreased (Fig. 8). The amount of resin penetration did not increase even at higher pressures, but the maximum penetration depth and with this the thickness of the interphase increased; this means that the penetrated resin was rather concentrated within the wood layer closest to the geometrical bond line.

Statistical differences concerning the influence of the applied pressure on the FIR values were observed between the two lower pressures for both tangential and radial directions as well as between the lowest and the highest pressures. At a given pressure level no significant difference exists between the two penetration directions.

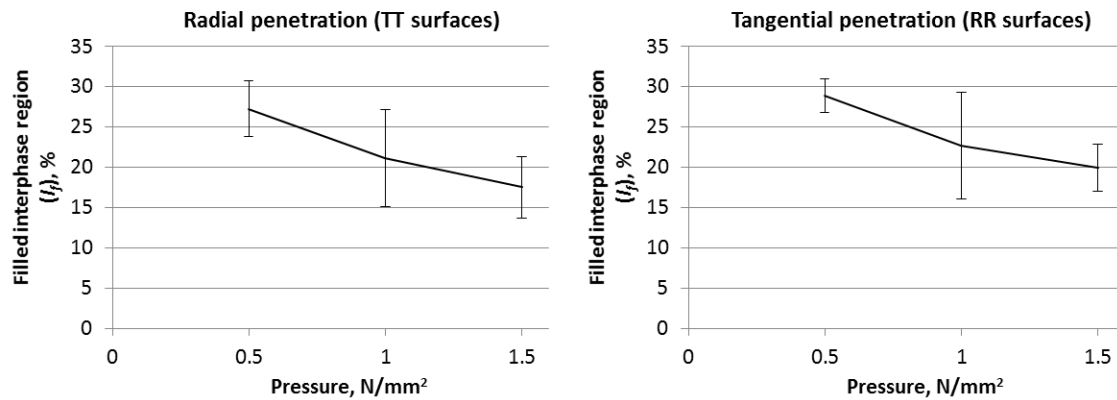


Fig. 8. Filled interphase region (I_f) (%) for poplar and UF resin I as a function of the specific pressure during the press process

Shear Strength of the Bond Produced at Various Pressures during the Press Cycle

Table 3 summarizes the various shear strengths measured when preparing the joints at various specific pressures during the press cycle.

Table 3. Summary of Shear Strengths for Joints Prepared at Various Pressures during the Press Cycle

Poplar UF I	Pressure	Shear Strength	Standard Deviation		Wood Failure	
	(N/mm ²)	(N/mm ²)	(N/mm ²)	(%)	(%)	(mm)
TT	0.5	6.8	1.1	17	77	0.63
	1.0	7.7	0.9	12	75	1.20
	1.5	7.2	0.8	12	86	2.50
RR	0.5	4.6	0.7	15	83	1.90
	1.0	6.8	0.8	12	81	1.50
	1.5	5.5	0.5	8	91	1.80

TT=Two tangential surfaces bonded (radial penetration)
RR=Two radial surfaces bonded (tangential penetration)

The shear strength was influenced by the applied pressure; increasing the pressure from 0.5 N/mm² to 1.0 N/mm² yielded a significant increase in shear strength for tangential penetration; an increase in radial penetration was less and also not statistically secured (Fig. 9). Further increased pressure during the production of the joints, however, did not yield higher shear strength, but rather a decrease in shear strength was observed. The highest values of the shear strength for both TT and RR samples were hence obtained with a medium pressure level of 1.0 N/mm².

The shear strengths between tangential surfaces (= radial direction of penetration) was always higher than for radial surfaces (= tangential direction of penetration) with a statistically secured difference at the lowest and at the highest pressure level and showed the significant influence of the bonding surface (direction of penetration).

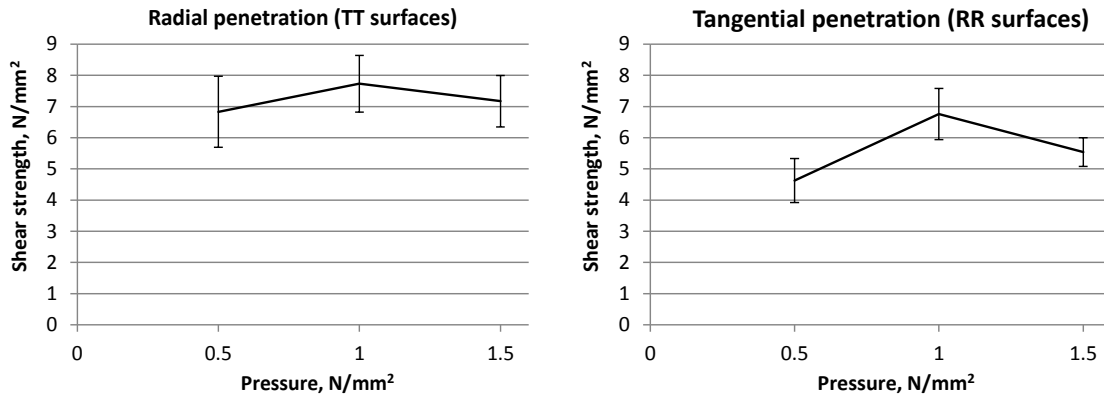


Fig. 9. Shear strength of joints made from poplar and UF resin UF I as a function of the specific pressure during the press process; results are shown for radial penetration (TT surfaces bonded) and for tangential penetration (RR surfaces bonded)

The increase of the shear strength might be caused by several factors, such as higher contact between the wood surfaces, which yielded a thinner bond line; also, the fortification of the interphase may have helped to increase bond strength, as this was assumed to be a consequence of the deeper penetration of the resin into the wood tissue (Gavrilovic-Grmusca 2012a). The lowest pressure obviously did not provide an appropriate level of penetration and interlocking, whereas at the highest pressure the interphase region did not increase further based on the restricted maximum penetration depth, but the proportion of filled lumens in the interphase (filled interphase region I_f) decreased significantly. Additionally, the changes in the wood structure under high pressure, in combination with moisture (from the applied resin) and the press temperature may have induced mechanical damages at the interphase bonding region, representing a certain degree of *in situ* mechanical weak boundary layer, resulting in lower shear strength. However, shear strength is always linked to the influence of wood failure. Per definition, a “good” wood joint should show a failure zone in the adjacent wood and not in the interphase or even in the bond line itself. Weakening the wood structure close to the bond line, however, drives the failure zone into the interphase, where these changes in the wood structure occurred.

The proportion of wood failure was high in all investigated cases. For the two lower pressures, basically the same values were found (but slightly higher for tangential penetration); for the highest pressure level, the wood failure increased for both directions (again, slightly higher for the tangential direction). This is an interesting effect, because the shear strengths were lower for both directions under the highest pressure level compared with the maximum shear strength at the medium level; this means that the shear strengths and proportion of wood failure did not correlate. There are two potential reasons for this: (i) the wood failures are high anyhow, so small differences in the original wood structure can cause a variation in shear strength; (ii) at the highest pressure a certain deterioration of the wood structure has already happened; this means the wood failure increased, whereas the shear strength did not increase but even slightly decreased.

The average thickness of the wood failure increased for the radial penetration with increased pressure; similarly, the higher pressure also caused an increase in average and maximum penetration depth. For tangential penetration, this effect was not clearly seen. In both cases, however, the average thickness of the wood failure was in the same order

of magnitude as the thickness of the interphase. This at least means that penetration heavily affects shear strength as well as wood failure.

Fluorescence Confocal Laser Scanning Microscopy (CLSM) and Scanning Electron Microscopy (SEM)

Figure 10 shows a CLSM micro-photograph of the radial penetration of resin into poplar by optical sectioning through a certain thickness of the microtome samples (20 μm) and a merging of the resulting photographs into one three-dimensional picture. The adhesive can be sharply differentiated from the cell walls using the bright contrast between the bond line and the penetrated adhesive (appearing reddish) on the one side and the cell walls (appearing greenish) on the other side when adding Safranin as a staining agent to the adhesive. The photo shows that the adhesive penetrated into the vessels as well as into the surrounding wood fibers. Some of the vessels and fibers were completely filled with adhesive, some of them only partially.

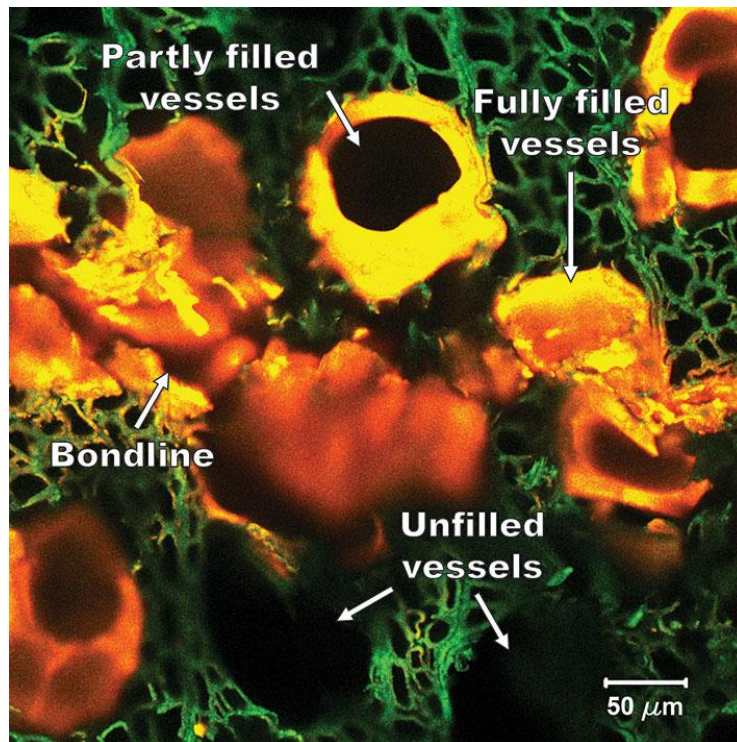


Fig. 10. Example of fluorescence confocal laser scanning microphotograph (CLSM) with the penetration of UF resin I into poplar: radial penetration, 1.0 N/mm² applied pressure

Figure 11 shows an SEM photograph of the radial UF I penetration into poplar, showing double vessels similar to ellipses. The longer axis was oriented in the radial direction, and the vessels were separated by a thin wall, which is characteristic for poplar. Again, the vessels were filled partly or fully with the adhesive, respectively, whereas the surrounding fibers contained none or only very little adhesive.

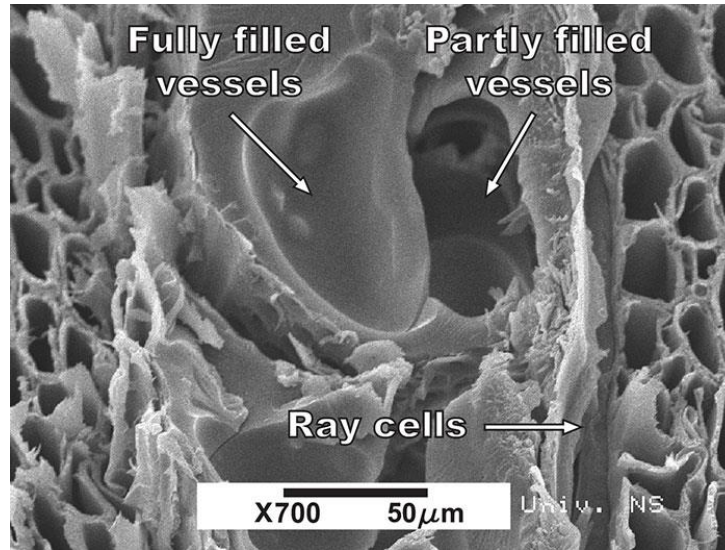


Fig. 11. Example of scanning electron microphotograph (SEM) with the penetration of UF resin I into poplar: radial penetration, 1.0 N/mm² applied pressure

CONCLUSIONS

1. Higher pressure applied during the press cycle increased the ability of the resin to penetrate more deeply into the wood tissue. Between the two lower pressure levels applied, a significant increase in penetration behavior was observed, whereas with further increased pressure this effect leveled out. The average penetration depth showed slightly higher tangential penetration at all pressure steps.
2. The interphase region, as it was determined by the maximum individual penetration depth, increased with higher applied pressure; both values were higher in the radial direction than in the tangential direction, which is contrary to d_{ap} ; this is the consequence of single flow paths enabling deep penetration in the radial direction; the resin was distributed in a broader layer compared with the tangential direction with its narrower interphase, but showed higher average penetration depth.
3. The average penetration depth of d_{ap} increased much more significantly than the maximum penetration depth of d_{max} ; the ratio of d_{max} to d_{ap} decreased significantly between the two lower pressure levels; this reflected the change in path flow diameters (vessel diameters) with decreasing cross-section, hindering extreme penetration; at the lowest specific pressure applied, the vessels remained rather unaltered and open for a certain portion of the resin to penetrate further away from the bond line.
4. The average size of filled lumens and rays within the interphase (A) decreased at higher pressures, which could have been caused by the change in the size primarily of the transport vessels, with their wide lumens and relatively thin walls. Additionally, due to the applied pressure, a stronger flow and hence, even squeezing out of the adhesive in the bond line occurred. In any case, it seems that the amount of resin penetration did not increase even at higher pressures, but the maximum penetration

depth and with this the thickness of the interphase increased; therefore also the filled interphase region as a proportion of the filled cells within the interphase decreased.

5. The bond strength, measured as the shear strength of the bonded joints, increased at moderate pressures but decreased again at high pressures. Additionally, the shear strength between tangential surfaces (depicting penetration in the radial direction) showed constantly higher values than those between the radial surfaces (tangential penetration).
6. Wood failure occurred in high proportions (>75%) for all of the test series. However, for both penetration directions, the wood failure increased under the highest pressure applied.

ACKNOWLEDGMENTS

The research work presented in this paper was financed by the Ministry of Educational and Science of the Republic of Serbia Project “Establishment of Wood Plantations Intended for Afforestation of Serbia” (TR 031041).

REFERENCES CITED

- Brady, E., and Kamke, F. (1988). "Effects of hot-pressing parameters on resin penetration," *Forest Prod. J.* 38(11–12), 63-68.
- Dunky, M. (2003). "Wood adhesives," in: *Handbook of Adhesive Technology*, 2nd Ed., Pizzi, A., and Mittal, K. L. (eds.), Marcel Dekker, New York, pp. 887-956.
- Edalat, H., Faezipour, M., Thole, V., and Kamke, F. A. (2014). "A new quantitative method for evaluation of adhesive penetration pattern in particulate wood-based composites: Elemental counting method," *Wood Sci. Technol.* 48(4), 703-712. DOI: 10.1007/s00226-014-0635-2
- Ellis, S., and Steiner, P. R. (1992). "Some effects of the chemical and physical characteristics of powdered phenol-formaldehyde resins on their adhesive performance," *Forest Prod. J.* 42(1), 8-14.
- European Standard: EN 205:2003, Adhesives — Wood adhesives for non-structural applications — Determination of tensile shear strength of lap joints.
- Evans, P. D., Morrison, O., Senden, T. J., Vollmer, S., Roberts, R. J., Limaye, A., Arns, C. H., Averdunk, H., Lowe, A., and Knackstedt, M. A. (2010). "Visualization and numerical analysis of adhesive distribution in particleboard using X-ray micro-computed tomography," *Int. J. Adhes. Adhes.* 30(8), 754-762. DOI: 10.1016/j.ijadhadh.2010.08.001
- Gavrilovic-Grmusa, I., Miljković, J., and Điporović-Momčilović, M. (2010a). "Influence of the degree of condensation on the radial penetration of urea formaldehyde adhesives into Silver Fir (*Abies alba* Mill.) wood tissue," *J. Adhesion Sci. Technology* 24(8-10), 1437-1453. DOI: 10.1163/016942410X501034
- Gavrilovic-Grmusa, I., Dunky, M., Miljković, J., and Điporović-Momčilović, M. (2010b). "Radial penetration of urea-formaldehyde adhesive resins into beech (*Fagus Moesiaca*)," *J. Adhes. Sci. Technol.* 24(8-10), 1753-1768. DOI: 10.1163/016942410X507812

- Gavrilovic-Grmusa, I., Dunky, M., Miljković, J., and Điporović-Momčilović, M. (2012a). "Influence of the degree of condensation of urea-formaldehyde adhesives on the tangential penetration into beech and fir and on the shear strength of the adhesive joints," *Eur. J. Wood Wood Prod.* 70(5), 655-665. DOI: 10.1007/s00107-012-0599-6
- Gavrilovic-Grmusa, I., Dunky, M., Miljković, J., and Điporović-Momčilović, M. (2012b). "Influence of the degree of condensation of urea-formaldehyde adhesive on radial and tangential penetration into poplar the shear strength of adhesive joints," *Holzforschung* 66(7), 849-856. DOI: 10.1515/hf-2011-0177
- Gavrilovic-Grmusa, I., Standfest, G., Petutschnigg, A., and Dunky, M. (2012c). (not published)
- Gindl, W., Zagar-Yaghubi, F., and Wimmer, R. (2003). "Impregnation of softwood cell walls with melamine-formaldehyde resin," *Biores. Technol.* 87(3), 325-330. DOI: 10.1016/S0960-8524(02)00233-X
- Hass, P., Falk, W., Stampanoni, M., Kaestner, A., and Niemz, P. (2009). "Penetration pathway of adhesives into wood," *Proc. Int. Conf. Wood Adhesives 2009*, Lake Tahoe, CA.
- Hass, P., Wittel, F. K., Mendoza, M., Herrmann, H. J., and Niemz, P. (2012). "Adhesive penetration in beech wood: Experiments," *Wood Sci. Technol.* 46(1-3), 243-256. DOI: 10.1007/s00226-011-0410-6
- Johnson, S. E., and Kamke, F. A. (1992). "Quantitative analysis of gross adhesive penetration in wood using fluorescence microscopy," *J. Adhes.* 40(1), 47-61. DOI: 10.1080/00218469208030470
- Kamke, F. A., Nairn, J. A., Muszynski, L., Paris, J. L., Schwarzkopf, M., and Xiao, X. (2014). "Methodology for micromechanical analysis of wood adhesive bonds using X-ray computed tomography and numerical modeling," *Wood Fiber Sci.* 46(1), 15-28.
- Konnerth, J., Harper, D., Lee, S.-H., Rials, T. G., and Gindl, W. (2008). "Adhesive penetration of wood cell walls investigated by scanning thermal microscopy (SThM)," *Holzforschung* 62(1), 91-98. DOI: 10.1515/HF.2008.014
- Mahrdt, E., Stoeckel, F., van Herwijnen, H. W. G., Mueller, U., Kantner, W., Moser J., and Gindl-Altmutter, W. (2015). "Light microscopic detection of UF adhesive in industrial particle board," *Wood Sci. Technol.* 49(3), 517-526. DOI: 10.1007/s00226-015-0715-y
- Marra, A. (1992). *Technology of Wood Bonding Principles in Practice*, Van Nostrand Reinhold, New York.
- Modzel, G., Kamke, F. A., and De Carlo, F. (2011). "Comparative analysis of a wood: Adhesive bondline," *Wood Sci. Technol.* 45(1), 147-158. DOI: 10.1007/s00226-010-0304-z
- Niemz, P., Mannes, D., Lehmann, E., Vontobel, P., and Haase, S. (2004). "Untersuchungen zur Verteilung des Klebstoffes im Bereich der Leimfuge mittels Neutronenradiographie und Mikroskopie," *Holz Roh Werkst.* 62(6), 424-432. DOI 10.1007/s00107-004-0515-9
- Nuryawan, A., Park, B. -D., and Singh, A. P. (2014). "Penetration of urea-formaldehyde resins with different formaldehyde/urea mole ratios into softwood tissues," *Wood Sci. Technol.* 48(5), 889-902. DOI: 10.1007/s00226-014-0649-9
- Paris, J. L., Kamke, F. A., Nairn, J. A., Schwarzkopf, M., and Muszynski, L. (2013). "Wood-Adhesive Penetration: Non-destructive, 3D visualization and quantification," *Proc. Int. Conf. Wood Adhesives 2013*, Toronto.

- Paris, J. L., Kamke, F. A., Mbachu, R., and Gibson, S. K. (2014). "Phenol formaldehyde adhesives formulated for advanced X-ray imaging in wood-composite bondlines," *J. Mater. Sci.* 49(2), 580-591. DOI: 10.1007/s10853-013-7738-2
- Pizzi, A. (1999). "On the correlation equations of liquid and solid ^{13}C -NMR, thermomechanical analysis, T_g , and network strength in polycondensation resins," *J. Appl. Polym. Sci.* 71(10), 1703–1709
- Sernek, M., Resnik, J., and Kamke, F. A. (1999). "Penetration of liquid urea-formaldehyde adhesive into beech wood," *Wood Fiber Sci.* 3(11), 41-48.
- Singh, A., Dawson, B., Rickard, C., Bond, J., and Singh, A. (2008). "Light, confocal and scanning electron microscopy of wood-adhesive interface," *Microsc. Analy.* 22(3), 5-8.
- Singh, A. P., Nuryawan, A., Park, B. -D., and Lee, K. H. (2015). "Urea-formaldehyde resin penetration into *Pinus radiata* tracheid walls assessed by TEM-EDXS," *Holzforschung* 69(3), 303-306. DOI: 10.1515/hf-2014-0103
- Wang, W., and Yan, N. (2005). "Characterizing liquid resin penetration in wood using a mercury intrusion porosimeter," *Wood Fiber Sci.* 37(3), 505-513.
- White, M. S. (1977). "Influence of resin penetration on the fracture toughness of wood adhesive bonds," *Wood Sci.* 10(1), 6-14.

Article submitted: July 31, 2015; Peer review completed: October 16, 2015; Revised version received: December 13, 2015; Accepted: December 20, 2015; Published: January 20, 2016.

DOI: 10.15376/biores.11.1.2238-2255